Solar Energy Materials & Solar Cells 226 (2021) 111097

Contents lists available at ScienceDirect

Solar Energy Materials and Solar Cells

journal homepage: http://www.elsevier.com/locate/solmat

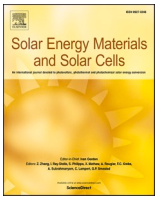

Nonselective etching of As and P based III–V solar cell heterostructures with aqueous solutions of HIO_3 and HCl

Marianna Raappana *, Tomi Koikkalainen, Ville Polojärvi, Arto Aho, Timo Aho, Riku Isoaho, Antti Tukiainen, Mircea Guina

Optoelectronics Research Centre, Physics Unit, Tampere University, P.O. Box 692, FI-33014, Tampere, Finland

ARTICLE INFO

Keywords:
Wet etching
Mesa etching
Nonselective etchant
Device fabrication
III–V heterostructures
Multijunction solar cell

ABSTRACT

Etching characteristics of lattice-matched GaInP/GaAs/GaInNAsSb heterostructures by aqueous solutions of iodic acid (HIO_3) and hydrochloric acid (HCl) is reported. The study aims at optimization of mesa fabrication process involved in the development of III–V multijunction solar cells. The effects of temperature, agitation, etchant composition, and illumination on the etching selectivity are investigated. Varying the etchant composition and agitation rate at room temperature results in various mesa sidewall morphologies, ranging from rough surfaces and significant undercut to smoother sidewall profiles with only minor undercut. Especially, the undercut emerging in the GaInNAsSb junction, as well as in the AlInP layers, was observed for several etching conditions. Increasing the etching temperature also caused an unwanted increase in the selectivity, whereas reducing the temperature below the room temperature enhanced remarkably the formation of smooth morphology. Illumination during the etching resulted in a severe undercut in the GaAs junction, due to an increased selectivity caused by photoetching. This points out the need of controlled illumination condition to avoid unwanted reactions in wet etching of such multijunction structures. The etching process resulting in the best morphology was used for electrical isolation of triple-junction GaInP/GaAs/GaInNAsSb solar cells. The good photovoltaic performance exhibited by these devices proves the suitability of the nonselective etch process in developing multijunction solar cells.

1. Introduction

Wet etching is a device processing method commonly used in optoelectronics industry owing to its scalability and low-cost nature compared to dry etching. While there are well-established selective etching processes with specific chemistries for a large variety of semiconductor materials [1], developments are continuously needed for novel heterostructures. This is necessary, in particular when etching of dissimilar materials with compositions requiring different etching chemistries are involved. Because etching is a result of a complex interplay between several parameters (e.g., etchant composition, etch duration, temperature, mass transfer, and initial semiconductor surface composition and structure [2]), thorough etching studies are needed to reveal the optimal processes for specific material systems and applications. Such optimization is especially required for the development of the next generation multijunction solar cells, comprising a wide range of III–As–P–N/GaAs and III–V/Ge alloys. Compared to other optoelectronic devices, the complexity of the process optimization for multijunction solar cells arises from the diversity of chemical properties of the semiconductor alloys involved.

Typical device architecture of III–V solar cells makes use of mesa etching to achieve component isolation [3]. This step is crucial since poor mesa sidewalls might deteriorate the photovoltaic response by providing sites for nonradiative perimeter recombination, causing pronounced leakage currents [4,5]. This aspect becomes even more important for smaller components due to a higher perimeter-to-area ratio, which are also used in concentrated photovoltaic applications [4–7].

Ideally, mesa etching should result in well-defined devices with good morphology, that is, smooth facets preferably as steep as possible and with a minimal amount of undercut. Moreover, the mesa would be formed by using a nonselective, well-controllable wet etchant owing to

* Corresponding author.
E-mail addresses: marianna.raappana@tuni.fi (M. Raappana), tomi.koikkalainen@gmail.com (T. Koikkalainen), ville.polojarvi@tuni.fi (V. Polojärvi), arto.aho@tuni.fi (A. Aho), timo.aho@tuni.fi (T. Aho), riku.isoaho@tuni.fi (R. Isoaho), antti.tukiainen@tuni.fi (A. Tukiainen), mircea.guina@tuni.fi (M. Guina).

https://doi.org/10.1016/j.solmat.2021.111097
Received 27 January 2021; Received in revised form 26 March 2021; Accepted 29 March 2021
Available online 13 April 2021

its practical simplicity as it enables a single-step etching process via immersion into an etchant solution for a specified time period. The challenge of using such a nonselective wet etchant for heterostructures incorporating different III–V alloys lies in the fact that etching of As and P based alloys are typically done with different etchants [1]. Etchants incorporating acids, such as H_2SO_4, H_3PO_4, HNO_3, and HF, or NH_3 base are traditionally used for arsenides whereas phosphides can be etched with HCl and HBr based etchants. However, nonselective etchants for III–V multijunction solar cells incorporating As and P based materials have been reported [8–10], yet more convenient, stable, and nontoxic methods need to be developed. In particular, this is valid for the next generation of solar cells with four or more absorber materials (i.e., junctions), including novel heterostructures, such as GaInNAsSb alloys, also with high N content [11,12]. To this end, etchants containing iodic acid (HIO_3) and hydrochloric acid (HCl) are a potential choice for their reported nonselective nature [13,14]. In this etchant system, HIO_3 acts as an oxidizer, while HCl dissolves the oxidized species [13]. Furthermore, this etchant system is not suitable only for heterostructures in multijunction solar cells but also for semiconductor heterostructures used in various optoelectronic devices.

Here, we report on the results of the etching of III–V alloys in multijunction solar cell structures by aqueous solutions containing HIO_3 and HCl. The effects of temperature, agitation, etchant composition, and illumination on the etching are studied, with the emphasis on the nonselectivity of the etching process. The quality of the etching was evaluated in terms of surface morphology and etch rates were determined by measuring the etching depth. The functionality of the etching was tested by fabricating and measuring multijunction solar cells.

2. Experimental

2.1. Sample description

The triple-junction GaInP/GaAs/GaInNAsSb solar cell structure consisting of various p- and n-doped layers of As and P based materials were grown lattice-matched on *p*-GaAs(100) substrate using a Veeco GEN20 plasma-assisted solid source molecular beam epitaxy (MBE) system. A more detailed description of the MBE growth of dilute nitride solar cells can be found in Ref. [15]. The total thickness of the epitaxial layers was below 10 μm. A schematic of the sample structure is depicted in Fig. 1. Etching samples did not have contact metallization.

2.2. Etching experiments

A patterned positive-tone photoresist (AZ 6632 Photoresist, Clariant GmbH) was used as an etching mask. Etching experiments were conducted in an open glass beaker with a magnetic stirrer. The samples were immersed into the etchant with the front surface facing towards the etchant flow to ensure an effective mass flow. The etchant components of HIO_3:HCl:H_2O solutions are reported in volume ratios of 0.4 M HIO_3, 37 m-% HCl, and deionized water.

In the first sample set, both the HIO_3 to HCl ratio and the dilution of the solution were varied in order to find proper etchant compositions. In addition, the etching time was varied, and some samples were etched sequentially to etch through all the epitaxial layers. In order to study the effect of agitation on the etching, magnetic stirring was applied with the rates of 0, 250, 500, 900, and 1300 rpm. Etching was conducted in ambient laboratory lighting. In the second sample set, etching experiments were conducted at various temperatures, ranging from −18.5 °C to 45 °C, in order to study the effect of temperature on the etching in ambient laboratory lighting.

Since light is known to induce selective etching [16], the susceptibility of the etchant system to photoinduced undercutting was investigated under different illumination conditions. Thus, in the third set, the effect of illumination on the etching was studied by performing experiments in the dark, in ambient led laboratory lighting, and under direct illumination from a 1000 lm flashlight (Mega 1000 LED, Airam) with a 10 W Cree white light led source.

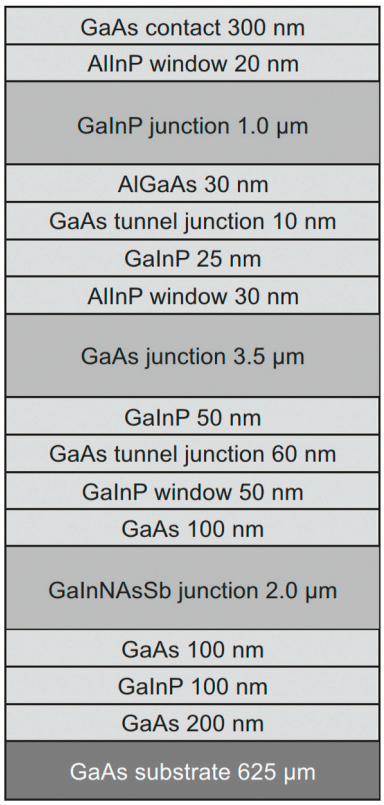

Fig. 1. A schematic drawing of the solar cell structure.

Samples are named in respect of the etching parameters. For example, **sample $C_{1:3:3}$-T_{20}-R_{900}** refers to the sample that was etched using HIO_3:HCl:H_2O with the composition (**C**) of 1:3:3, at the temperature (**T**) of 20 °C, and with the agitation rate (**R**) of 900 rpm. To calculate the etch rates, etch depths were measured with a stylus profilometer Dektak® 150 Surface Profiler (Veeco). In addition, the samples were cleaved into sections to investigate the cross-sectional profiles of the etched mesa sidewalls by Carl Zeiss Ultra-55 scanning electron microscope (SEM). The undercut is measured for a specific heterostructure layer relative to the neighboring layers, caused by unwanted selectivity of the etchant.

2.3. Solar cell fabrication and characterization

Finally, mesa structures of size 2 × 2 mm^2 were fabricated on triple-junction GaInP/GaAs/GaInNAsSb solar cells with the optimized etchant composition and process parameters that were selected based on the etching experiments. As a reference, similar solar cells were fabricated with the mesa etched by inductively coupled plasma (ICP) etching. The components included also front and back metal contacts and a double-layer TiO_x/SiO_y antireflection coating (ARC) deposited by electron beam evaporation. Prior to ARC deposition, contact GaAs layer was removed by selective wet etching. In order to characterize the device performance, light-biased current-voltage (IV) measurements were conducted using a 7 kW TriSol solar simulator (OAI Corporation) under AM0 spectrum (1366 W/m^2).

3. Results and discussion

3.1. Etchant characterization

Here, the discussion is divided into three sections: 1) The

composition and agitation related results at room temperature (20 °C), 2) the etching behavior at different temperatures, and 3) the effect of illumination on the etching.

3.1.1. The effect of composition and agitation

Varying the etchant composition and agitation rate at room temperature resulted in various mesa sidewall morphologies ranging from very poor morphology with rough surfaces and significant undercut to better morphologies characterized by smoother sidewall profiles with only minor undercut. The results are summarized in Fig. 2.

The smoothest sidewall morphology with the least amount of undercut at room temperature was achieved with an etchant composition of 1:1:1 HIO_3:HCl:H_2O. This corresponds to the concentrations of 0.13 M HIO_3 and 4.0 M HCl, with the stoichiometric ratio of 1:30 HIO_3:HCl. With this, higher agitation rates resulted in better sidewall morphologies, as seen in samples $C_{1:1:1}$-T_{20}-R_{1300} (Fig. 2a) and $C_{1:1:1}$-T_{20}-R_{900} (Fig. 2b). The sidewall profiles are smooth, round, and isotropic, typical profiles resulting from diffusion-controlled etching [17]. The lower agitation rate in sample $C_{1:1:1}$-T_{20}-R_{250} (Fig. 2c) produces a seemingly rougher etching result with some debris remaining on the etched surface, but still it creates a round, isotropic profile. Due to a lower agitation rate, mass transport is insufficient for etch products to diffuse away from the surface. This phenomenon is pronounced in sample $C_{1:1:1}$-T_{20}-R_0 (Fig. 2d) without agitation, where a high amount of etch debris is observed. In addition, a significant, 6.4 μm undercut has emerged in the GaInNAsSb junction together with noticeable undercut in the AlInP window layers and revealing also crystallographic facets and thus a kinetically controlled nature of the etching. Thus, with insufficient agitation, unwanted selectivity between different semiconductor materials seems to arise with this etchant. In addition, diluting the 1:1:1 ratio further to 1:1:10 leads to a significant amount of undercut in the GaAs junction, as shown in Fig. 2e. This behavior underlines the importance of the etchant dilution when it comes to the selectivity of the etchant towards different semiconductor materials.

In order to look for nonselective etching for all the semiconductor alloys present in the multijunction structure, the ratio of HIO_3 to HCl was varied in the vicinity of the ratio 1:1. Thus, we used ratios of 3:2:3, 3:1:3, 2:3:3, and 1:3:3 with the agitation rates of 250, 500, and 900 rpm. Similar to the 1:1:1 etchant composition, also these etchants resulted in better sidewall morphology with faster agitation. Thus, Fig. 2 presents

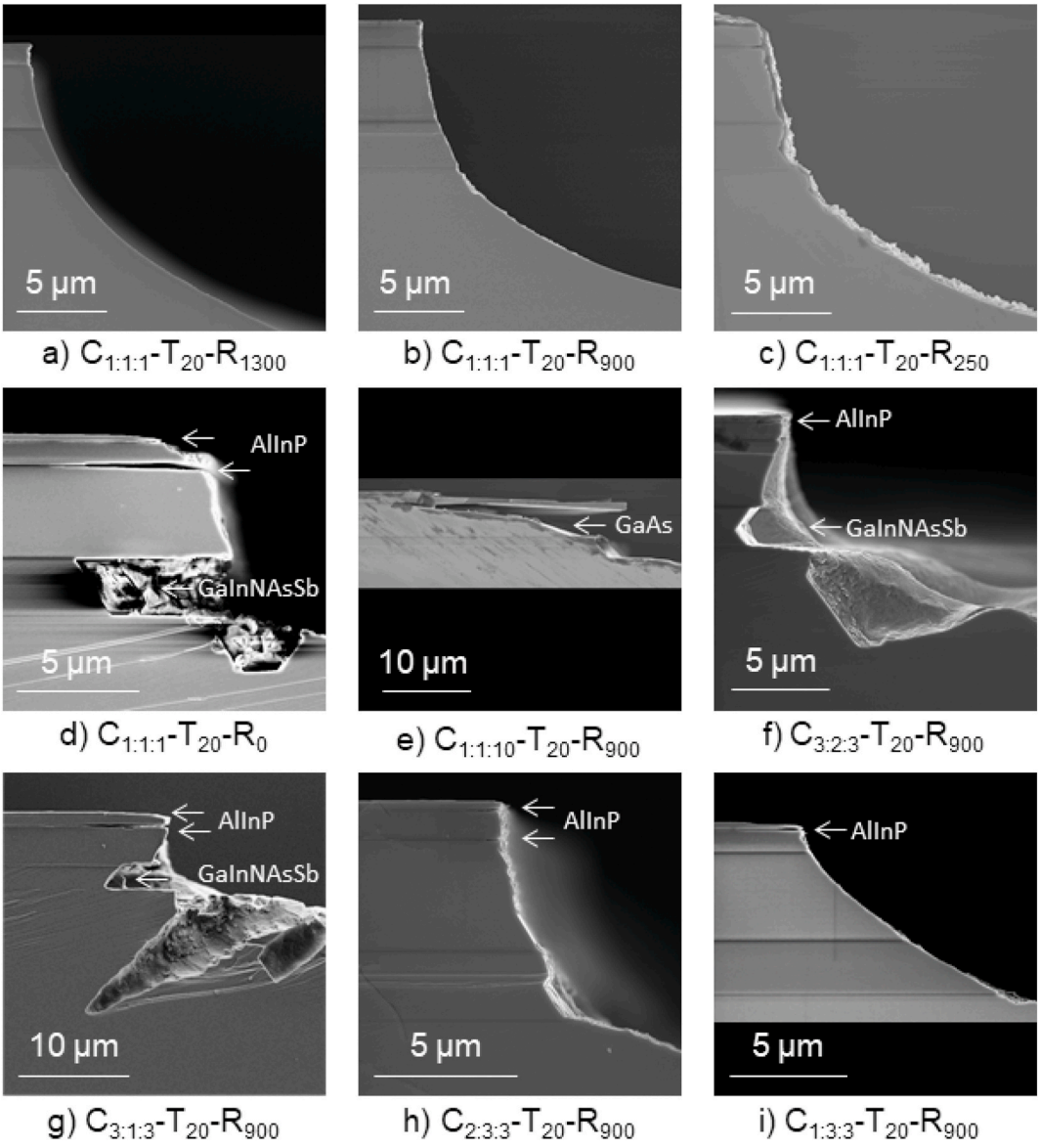

Fig. 2. SEM images of mesa sidewalls of the samples etched with different etchant compositions and agitation rates at room temperature in ambient laboratory lighting.

only the samples with the agitation rate of 900 rpm.

Reducing the HCl content, i.e., changing the HIO_3 to HCl ratio from 1:1 to 3:2 (Figs. 2f) and 3:1 (Fig. 2g), produced very uneven sidewall morphologies, with the effect being more pronounced with the lower HCl content. Selectivity is increased between different III–V semiconductors as there is serious undercut in the GaInNAsSb junction (1.5 μm for 3:2 and 4.8 μm for 3:1) as well as in the AlInP window layers. In addition, the overall etching result seems very undulating in sample $C_{3:2:3}$-T_{20}-R_{900}, while in sample $C_{3:1:3}$-T_{20}-R_{900} the bottom surface of the etched mesa exhibits drilled-like cavities. Therefore it can be stated that lowering the HCl content degrades the etching morphology and increases the unwanted selectivity. On the other hand, reducing the HIO_3 content, i.e., changing the HIO_3 to HCl ratio from 1:1 to 2:3 (Figs. 2h) and 1:3 (Fig. 2i), produces remarkably smoother mesa facets than with the reduced HCl content but still some amount of undercut in the AlInP window layers is observed. In addition, the sidewall profile of 1:3 ratio has more gentle slope than the ratio 2:3, which is an unwanted feature. Thus, since the etchant ratio of 1:1 produces smooth mesa sidewalls with no indication of selectivity, it is deemed as providing better etching results.

Etch rates vary depending on the etchant composition and the agitation rate. In general, higher agitation rates resulted in faster etching, owing to a more efficient mass transport due to a reduced thickness of the diffusion layer on the etched surface [18,19]. The 1:1:1 etchant showed the highest etch rates compared to the other etchant compositions, exceeding the etch rate of 3 μm/min with agitation rates of 1300 rpm and 900 rpm. The etch rates of the other compositions remained close to 1 μm/min with the agitation rate of 900 rpm. These etch rates are within a practical range from the fabrication point of view since etching through the whole mesa structure of 10 μm takes only a few minutes.

3.1.2. The effect of temperature

In order to study the temperature dependence of the etching process, 1:1:1 etchant was applied also at the elevated temperature of 45 °C and at lowered temperatures of 1 °C, −4.5 °C, −9 °C, and −18.5 °C in addition to room temperature. The resulting sidewall morphologies are shown in Fig. 3.

Compared to the sidewall profile etched at room temperature with the agitation rate of 900 rpm (Fig. 3b), at 45 °C a significant, 5.6 μm undercut has developed in the GaInNAsSb junction and the GaAs substrate, leaving the surface full of debris and revealing crystal planes underneath, as seen in Fig. 3a. In addition, heavy undercut is seen in the AlInP window layers. Thus, it can be stated that higher etching temperature increases the selectivity of the 1:1:1 etchant. It remains unclear whether the debris is unetched semiconductor material or etch products.

For etching below room temperature, the etch morphology is remarkably enhanced compared to the elevated temperature of 45 °C, as seen in Fig. 3c–f. In general, the sidewalls appear rather smooth, steep, and free of undercut and debris, showing also crystallographic facets of the semiconductor layers. The etch profiles seem to be footed, i.e., having quite straight upper part with footed lower part. At lower temperatures, −9.5 °C and −18.5 °C, more crystallographic facets are seen, pointing towards an increased kinetically controlled nature of the etching of some material layers. This observation is in line with the theory, according to which chemical reactions are temperature-dependent, as dictated by Arrhenius equation [19]. Thus, the reaction kinetics start to dominate over diffusion control, becoming the rate-limiting step in the etching at lower temperatures for some of the materials in the multijunction structure. The etching at temperatures of

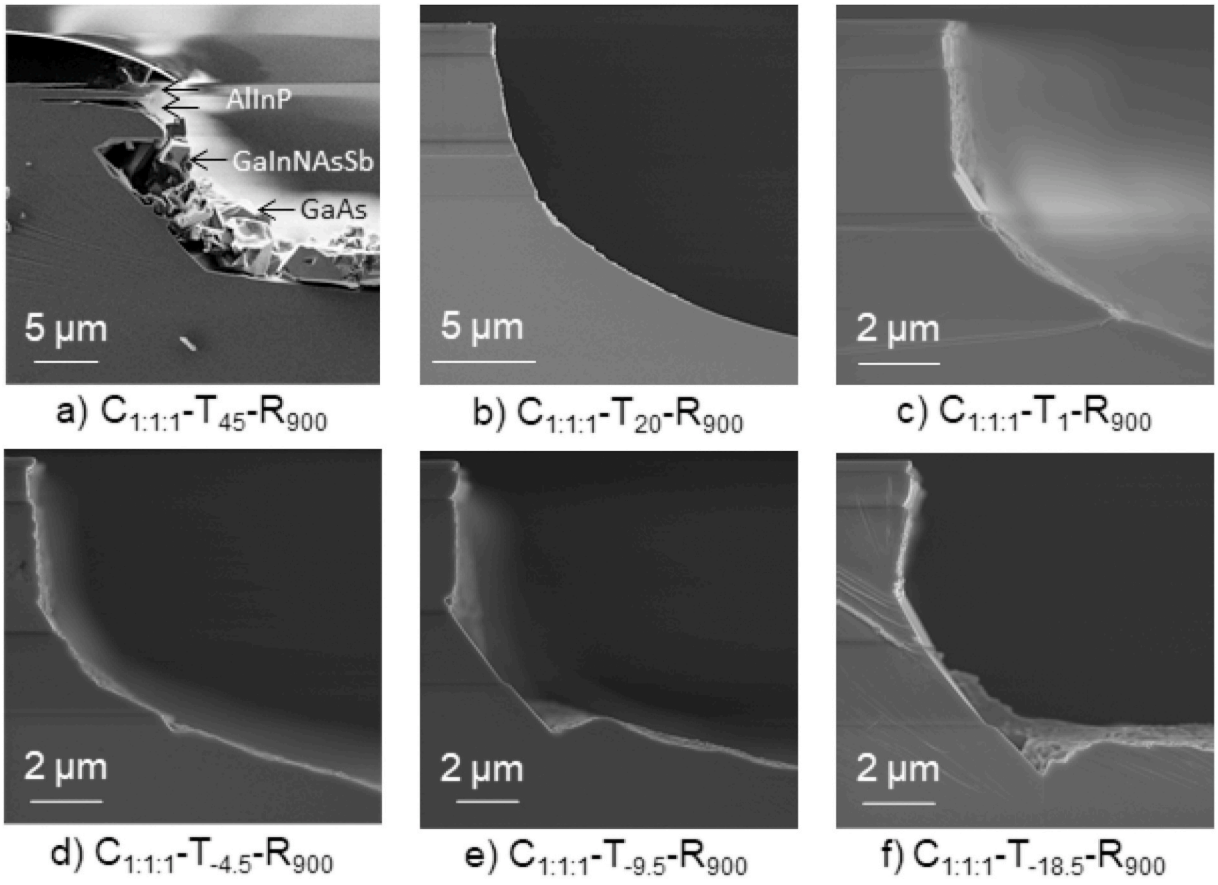

Fig. 3. SEM images showing the sidewall morphologies of the samples etched with the 1:1:1 etchant composition at different temperatures in ambient laboratory lighting.

1 °C and −4.5 °C reveal less crystallographic facets and thus resemble more the isotropic profile seen in the room temperature etching.

Based on the etch rate data at different temperatures, one can derive the activation energy (E_a) of the etching process and study the etching mechanism with the help of the relation

$$\ln v_{etch} = -(E_a/R)(1/T) + \ln A, \quad (1)$$

which is derived from the Arrhenius equation. Here, v_{etch} is the etch rate, R the ideal gas constant, T the etching temperature, and A a pre-exponential factor. From Equation (1), activation energy values can be derived for the etching of one-material systems with specific crystal directions [20,21]. However, since we now have a multijunction structure, the specific activation energy values for every material present cannot be determined, but instead we can derive a combined value for this etching system that can be used as a tool for evaluating the etching mechanism. The natural logarithm of the etch rate was plotted against the reciprocal of the etching temperature presented in Kelvin, which is shown in Fig. 4 together with the etch rate data and the derived equation from a linear fit made on data points. The etch rate at 45 °C significantly deviates from the trend, which together with the observed sidewall undercut indicates that the etch mechanism in this case is clearly different compared to the other etchings. For this reason, this data point was ignored from the fitting.

Since the slope of the linear fit equals to $-E_a/R$ according to Eq. (1), the value of 26.5 kJmol^{-1} ± 4.0 kJmol^{-1} was obtained for the activation energy for this etching system. It should be noted that this value is an averaged value for the whole multijunction structure and can thus be used only as an approximate. The derived value is well in line with the values from literature, according to which high activation energies, in the range of about 30–90 kJmol^{-1} refer to reaction rate limited process, whereas lower energies in the range of from 4 to 25 kJmol^{-1} refer to diffusion limited process [22]. The obtained value of E_a falls between these ranges, which is logical based on the observation that both crystal facets and isotropic features are present in Fig. 3.

3.1.3. The effect of illumination

In order to study the effect of illumination, tests with the 1:1:1 etchant were continued at room temperature using an agitation rate of 900 rpm in the dark, in ambient laboratory lighting, and under illumination. Fig. 5 shows the resulting sidewall profiles which have clear differences. The etch profile of sample $C_{1:1:1}$-T_{20}-R_{900}-D (Fig. 5a), which was etched in the dark, exhibits a similar isotropic etch profile as the corresponding sample ($C_{1:1:1}$-T_{20}-R_{900}) etched in ambient laboratory lighting (Fig. 5b). As a result, it can be said that for this particular etchant composition, the etching mechanism is the same in the dark and in ambient laboratory lighting, and no unwanted photoinduced selective etching occurs in ambient laboratory lighting.

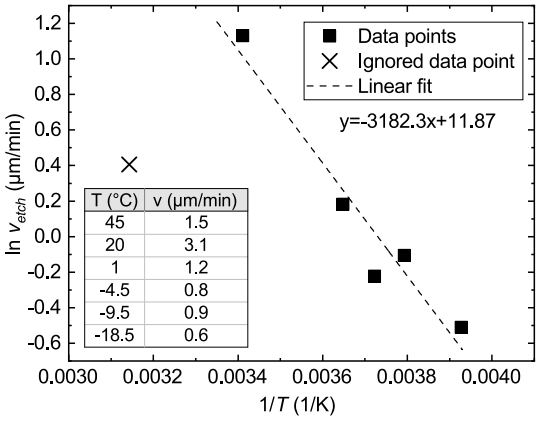

Fig. 4. Arrhenius plot where the natural logarithm of the etch rate is plotted as a function of the reciprocal of the temperature.

However, sample $C_{1:1:1}$-T_{20}-R_{900}-L, etched under direct illumination (Fig. 5c), exhibits a severe undercut in the GaAs junction, indicating that the selectivity of the etching has greatly increased due to illumination. There occurs now clearly also photoetching, in which electron-hole pairs are created in a semiconductor when the material is illuminated with photons equal to or higher than the band gap energy of the material; the photogenerated holes are supposed to oxidize the semiconductor while the electrons in the conduction band reduce the oxidizing agent of the etchant [16]. In this case, owing to the use of a white light led sources, the illumination spectrum involves mainly photons in the wavelength range of about 400–700 nm, i.e., photons with energy within the GaInP and GaAs band gap energy ranges. However, since the topmost contact GaAs layer filters out the wavelengths of the GaInP junction, the effect on GaAs etching is pronounced in the multijunction structure. Since the unwanted selectivity is increased so significantly, in order to obtain proper mesa sidewalls, etching under heavy illumination should be avoided. Nevertheless, a photoetching effect was shown, but in order to study the etching mechanism in more detail, the spectrum and the intensity of the illumination should be well known. Now it can be stated that since the etching is affected significantly by illumination, lighting conditions should be taken carefully into account in order to avoid any unwanted selectivity while etching multijunction structures.

Etch rates for comparable samples in the dark, in ambient lighting, and under illumination were 2.9 μm/min, 2.7 μm/min, and 2.5 μm/min, respectively. The lowest etch rate of the illuminated sample could be partly explained by a more pronounced lateral etching component due to the formed undercut.

3.2. Solar cell performance

Based on the etching studies, mesa structures were formed in triple-junction GaInP/GaAs/GaInNAsSb solar cells with the 1:1:1 HIO_3:HCl:H_2O etchant solution at 2 °C, using 900 rpm agitation in ambient laboratory lighting. Altogether 12 components were fabricated with the HIO_3:HCl:H_2O etchant and as a reference, 13 components using ICP etching, which is known to provide a well-functioning mesa isolation. The components have four slightly different front contact grid layouts leading to four different active areas of the solar cells. These are denoted as Cells 1–4. The figures of merit derived from the IV measurements of the solar cells are presented in Table 1. The values are averaged between the parallel cell components. The IV curves of the best performers of each Cell 1–4 together with their references are depicted in Fig. 6.

In general, the values for the HIO_3:HCl:H_2O etched solar cells shown in Table 1 are very close to the refence values. Individual parameters have the highest values within both etchings, so no real differences can be concluded in their electrical performance. Small variance in the performance can be explained as a normal outcome of the fabrication process. The fill factor values reveal a good performance, with the values of over 80% for all the cells. This is also proved by the IV curves, which has close to ideal shape with no major sign of shunting behavior, thus indicating a good quality of the fabrication.

In order to further compare the different etching methods, average values using active areas were derived for all the Cells 1–4 and their references. These values are shown in Table 2. The HIO_3:HCl:H_2O etched solar cells show higher average values in V_{OC} and fill factor, whereas the reference cells show higher average values in conversion efficiency and J_{SC}. However, when comparing the percentual differences in the average values to reference values, the differences are only marginal: 1.0%, +0.1%, −0.7%, and +0.1% for efficiency, V_{OC}, J_{SC}, and fill factor, respectively. Moreover, the values of conversion efficiency and J_{SC} are assumingly slightly underestimated for the HIO_3:HCl:H_2O etched solar cells, since mesa etching by wet etching produces smaller mesa areas compared to ICP etching due to the undercutting. As a conclusion, it can be stated that a successful mesa isolation was obtained with the HIO_3:HCl:H_2O etchant solution, producing solar cells with comparable

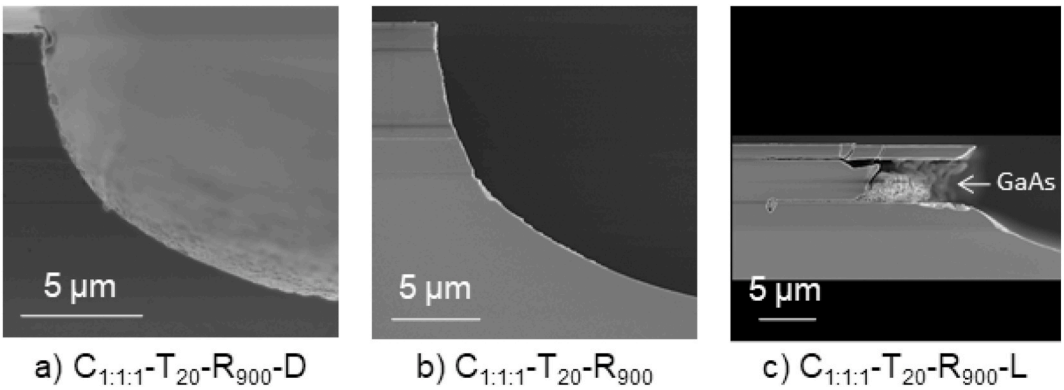

Fig. 5. SEM images of the sidewalls of the samples etched with the 1:1:1 etchant composition a) in the dark, b) in ambient laboratory lighting, c) and as illuminated.

Table 1
IV characteristics of the solar cells. Presented values are averaged values between the parallel cell components. The highest values between the HIO_3:HCl:H_2O etched solar cells and their reference solar cells are marked in bold.

Solar cell ID	Efficiency (%)	V_{OC} (V)	J_{SC} (mA/cm^2)	Fill factor (%)
1	**19.79**	2.569	**13.01**	80.9
1-Ref	19.76	**2.580**	12.91	**81.1**
2	**20.26**	**2.590**	13.07	**81.8**
2-Ref	20.19	2.580	**13.16**	81.2
3	20.54	**2.591**	13.28	**81.5**
3-Ref	**20.69**	2.583	**13.47**	81.2
4	21.13	**2.591**	13.62	81.8
4-Ref	**21.63**	2.587	**13.92**	**82.0**

electrical performance to the reference solar cells.

4. Conclusions

The etching of III–V alloys in GaInP/GaAs/GaInNAsSb solar cell structures by aqueous solutions containing HIO_3 and HCl was studied, with the focus being on the effects of temperature, agitation, etchant composition, and illumination on the etching. Depending on the etching conditions, sidewall morphologies varied from very smooth, round, and isotropic to poor-quality sidewall facets with a large amount of undercut. The main trends originating from different etching conditions are summarized in Table 3.

It can be stated that the selectivity of the HIO_3:HCl:H_2O etchant depends largely on the used etching conditions. Especially, the GaInNAsSb junction and AlInP window layers seem to be prone to faster etching with several etching conditions, e.g., with the 1:1:1 composition at the elevated temperature, with no agitation at room temperature, and when the HCl content is reduced by changing the HIO_3 to HCl ratio from 1:1 to 3:2 and 3:1. The susceptibility of Al containing III–V layers to undercutting has also been previously reported [14]. In addition, unwanted selectivity caused by photoetching became prominent in the GaAs junction when etching was performed under illumination from a white led. Such illumination related unwanted reactions need to be taken into account when wet etching is done for multijunction structures.

Table 2
The average values of the IV characteristics of the solar cells. The highest values are marked in bold. Average values for efficiency and J_{SC} are calculated using active area of the solar cells.

Solar cell ID	Efficiency (%)	V_{OC} (V)	$J_{SC,\ active}$ (mA/cm^2)	Fill factor (%)
Average Cells 1–4	20.6	**2.585**	13.4	**81.5**
Average Ref. Cells 1–4	**20.8**	2.582	**13.5**	81.4

Table 3
Summary of the trends observed in the mesa etching of GaInP/GaAs/GaInNAsSb solar cells by HIO_3:HCl:H_2O solutions.

Parameter	Parameter increased	Parameter decreased
Agitation	Improves sidewall morphology	Degrades sidewall morphology: induces undercutting and debris
HIO_3 to HCl ratio	Degrades sidewall morphology: undulation and holes emerged	Good sidewall morphology maintained: resembles the 1:1 ratio
Temperature	Degrades sidewall morphology: induces undercutting and debris	Improves sidewall morphology: isotropic and crystallographic features emerged
Illumination	Degrades sidewall morphology: undercut in GaAs junction	Good sidewall morphology maintained: resembles the ambient lighting

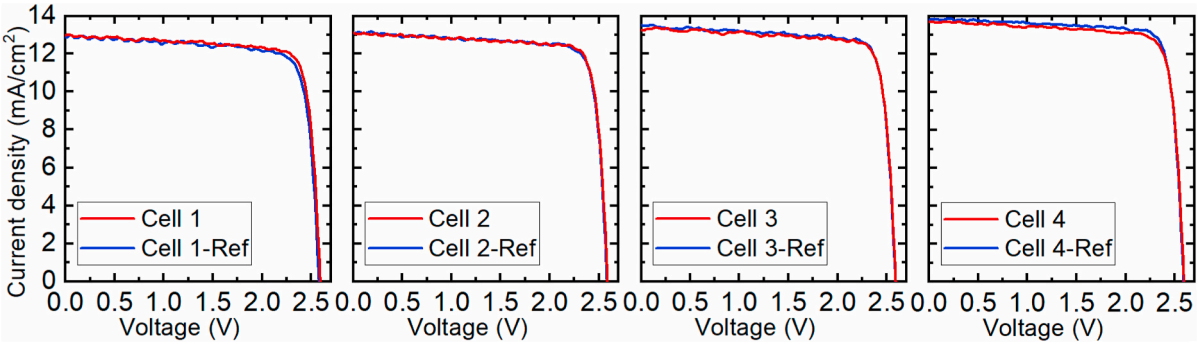

Fig. 6. IV curves of the best individual performers of the fabricated Cells 1–4 and their references.

In conclusion, the best sidewall morphologies were obtained with the 1:1:1 composition with high agitation (i.e., 900 rpm or 1300 rpm) both at room temperature and at lower temperatures in ambient laboratory lighting, as well as at room temperature in the dark. Based on this, we chose the etching conditions for fabricating the mesa structures of the actual solar cell components to be the 1:1:1 HIO_3:HCl:H_2O solution at 2 °C with 900 rpm agitation in ambient laboratory lighting. Based on the IV characterization, solar cell performance was proven to be comparable to the reference solar cells etched with ICP. All the fabricated solar cells exhibited a fill factor value of over 80%, revealing a good quality of fabrication and mesa etching. As a conclusion, it can be stated that a successful mesa isolation was achieved with the HIO_3:HCl:H_2O etchant.

CRediT authorship contribution statement

Marianna Raappana: Conceptualization, Methodology, Validation, Investigation, Writing – original draft, Visualization, Project administration, Writing – review & editing. **Tomi Koikkalainen:** Methodology, Validation, Investigation, Writing – review & editing. **Ville Polojärvi:** Conceptualization, Methodology, Supervision, Writing – review & editing. **Arto Aho:** Conceptualization, Resources, Supervision, Writing – review & editing. **Timo Aho:** Methodology, Investigation, Writing – review & editing. **Riku Isoaho:** Resources, Writing – review & editing. **Antti Tukiainen:** Supervision, Writing – review & editing. **Mircea Guina:** Supervision, Funding acquisition, Writing – review & editing.

Declaration of competing interest

The authors declare that they have no known competing financial interests or personal relationships that could have appeared to influence the work reported in this paper.

Acknowledgements

The work has been funded by the European Research Council under the "AMETIST" ERC Advanced Grant ERC-2015-AdG 695116. The work is also part of the Academy of Finland Flagship Program PREIN 320168. The authors would like to thank Arttu Hietalahti for his technical assistance. In addition, M. R. acknowledges personal support from The Finnish Foundation for Technology Promotion, Jenny and Antti Wihuri Foundation, and Walter Ahlström Foundation.

References

[1] A.R. Clawson, Guide to references on III–V semiconductor chemical etching, Mater. Sci. Eng. R 31 (2001) 1–438, https://doi.org/10.1016/S0927-796X(00)00027-9.
[2] F. Seker, K. Meeker, T.F. Kuech, A.B. Ellis, Surface chemistry of prototypical bulk II−VI and III−V semiconductors and implications for chemical sensing, Chem. Rev. 100 (2000) 2505–2536, https://doi.org/10.1021/cr980093r.
[3] A.L. López, V.M. Andreev, Concentrator Photovoltaics, first ed., Springer, 2007 https://doi.org/10.1007/978-3-540-68798-6.
[4] M. Ochoa, C. Algora, P. Espinet-González, I. García, 3-D modeling of perimeter recombination in GaAs diodes and its influence on concentrator solar cells, Sol. Energy Mater. Sol. Cells 120 (2014) 48–58, https://doi.org/10.1016/j.solmat.2013.08.009.
[5] A. Belghachi, S. Khelifi, Modelling of the perimeter recombination effect in GaAs-based micro-solar cell, Sol. Energy Mater. Sol. Cells 90 (2006) 1–14, https://doi.org/10.1016/j.solmat.2005.01.009.
[6] A. Ritou, P. Voarino, O. Raccurt, Does micro-scaling of CPV modules improve efficiency? A cell-to-module performance analysis, Sol. Energy 173 (2018) 789–803, https://doi.org/10.1016/j.solener.2018.07.074.
[7] P. Espinet-González, I. Rey-Stolle, M. Ochoa, C. Algora, I. García, E. Barrigón, Analysis of perimeter recombination in the subcells of GaInP/GaAs/Ge triple-junction solar cells, Prog. Photovolt. 23 (2015) 874–882, https://doi.org/10.1002/pip.2501.
[8] A. Turala, A. Jaouad, D.P. Masson, S. Fafard, R. Arès, V. Aimez, Isolation of III–V/Ge multijunction solar cells by wet etching, Int. J. Photoenergy (2013), https://doi.org/10.1155/2013/583867.
[9] V.S. Kalinovsky, E.A. Grebenshchikova, P.A. Dmitriev, N.D. Il'inskaya, E. V. Kontrosh, A.V. Malevskaya, A.A. Usikova, V.M. Andreev, Photoelectric characteristics of InGaP/Ga(In)As/Ge solar cells fabricated with a single-stage wet chemical etching separation process, AIP Conf. Proc. 1616 (2014) 326–330, https://doi.org/10.1063/1.4897088.
[10] M.F. Bennett, M. González, M.P. Lumb, M.K. Yakes, K.J. Schmieder, S. Tomasulo, J. Abell, J.R. Meyer, R.J. Walters, Development of wet etch processing for $In_xAl_{1-x}As_ySb_{1-y}$ solar cells grown on InP, in: IEEE 42nd Photovoltaic Specialist Conference, PVSC), 2015, pp. 1–4, https://doi.org/10.1109/PVSC.2015.7356353, 2015.
[11] M. Raappana, V. Polojärvi, A. Aho, J. Mäkelä, T. Aho, A. Tukiainen, P. Laukkanen, M. Guina, Wet etching of dilute nitride GaInNAs, GaInNAsSb, and GaNAsSb alloys lattice-matched to GaAs, Corrosion Sci. 136 (2018) 268–274, https://doi.org/10.1016/j.corsci.2018.03.018.
[12] R. Isoaho, A. Aho, A. Tukiainen, T. Aho, M. Raappana, T. Salminen, J. Reuna, M. Guina, Photovoltaic properties of low-bandgap (0.7–0.9 eV) lattice-matched GaInNAsSb solar junctions grown by molecular beam epitaxy on GaAs, Sol. Energy Mater. Sol. Cells 195 (2019) 198–203, https://doi.org/10.1016/j.solmat.2019.02.030.
[13] M. Zaknoune, O. Schuler, F. Mollot, D. Théron, Y. Crosnier, Nonselective wet chemical etching of GaAs and AlGaInP for device applications, J. Vac. Sci. Technol. B 16 (1998) 22–226, https://doi.org/10.1116/1.589783.
[14] O. Fidaner, M.W. Wiemer, V.A. Sabnis, E.N. Lucow, Method for Etching Multi-Layer Epitaxial Material, Pat. US 9263611 B2, 16.2.2016. Appl. No. 13/679922, 16.11.2012.
[15] A. Aho, V. Polojärvi, V.M. Korpijärvi, J. Salmi, A. Tukiainen, P. Laukkanen, M. Guina, Composition dependent growth dynamics in molecular beam epitaxy of GaInNAs solar cells, Sol. Energy Mater. Sol. Cells 124 (2014) 150–158, https://doi.org/10.1016/j.solmat.2014.01.044.
[16] W. Gomes, Wet etching of III–V semiconductors, in: H.S. Nalwa (Ed.), Handbook of Advanced Electronic and Photonic Materials and Devices, Academic Press, Burlington, 2001, pp. 221–256.
[17] A.G. Baca, C.I.H. Ashby, Fabrication of GaAs Devices, Bibliovault OAI Repository, the University of Chicago Press, 2005, https://doi.org/10.1049/PBEP006E.
[18] S.S. Tan, M. Ye, A.G. Milnes, Diffusion limited chemical etching effects in semiconductors, Solid State Electron. 38 (1995) 17–24, https://doi.org/10.1016/0038-1101(94)E0072-M.
[19] P.H.L. Notten, J.E.A.M. van den Meerakker, J.J. Kelly, Etching of III–V Semiconductors: an Electrochemical Approach, Elsevier Advanced Technology, Oxford, UK, 1991.
[20] C. Thomas, Y. Tamura, T. Okada, A. Higo, S. Samukawa, Estimation of activation energy and surface reaction mechanism of chlorine neutral beam etching of GaAs for nanostructure fabrication, J. Phys. D 47 (2014), 275201, https://doi.org/10.1088/0022-3727/47/27/275201.
[21] S. Tan, R. Boudreau, M.L. Reed, Anisotropic etching of silicon on {111} and near {111} planes, Sensor. Mater. 13 (2001) 303–313.
[22] S. Franssila, Introduction to Microfabrication, John Wiley & Sons, 2004.